

Title	Cardioprotective effect of fingolimod against calcium paradox-induced myocardial injury in the isolated rat heart
Authors	Alatrag, Fatma;Amoni, Matthew;Kelly-Laubscher, Roisin;Gwanyanya, Asfree
Publication date	2021-09-24
Original Citation	Alatrag, F., Amoni, M., Kelly-Laubscher, R. and Gwanyanya, A. (2021) 'Cardioprotective effect of fingolimod against calcium paradox-induced myocardial injury in the isolated rat heart', Canadian Journal of Physiology and Pharmacology, 100(2), pp. 134-141. doi: 10.1139/cjpp-2021-0381
Type of publication	Article (peer-reviewed)
Link to publisher's version	10.1139/cjpp-2021-0381
Rights	© 2021, the Authors. Published by Canadian Science Publishing.
Download date	2025-08-01 13:04:33
Item downloaded from	<a href="https://hdl.handle.net/10468/12566">https://hdl.handle.net/10468/12566</a>



# Canadian Journal of Physiology and Pharmacology

## Cardioprotective effect of fingolimod against calcium paradox-induced myocardial injury in the isolated rat heart

Journal:	<i>Canadian Journal of Physiology and Pharmacology</i>
Manuscript ID	cjpp-2021-0381.R2
Manuscript Type:	Article
Date Submitted by the Author:	08-Sep-2021
Complete List of Authors:	Alatrag, Fatma; University of Cape Town, Human Biology Amoni, Matthew; University of Cape Town, Human Biology Kelly-Laubscher, Roisin; University of Cape Town, Biological Sciences; University College Cork, Department of Pharmacology and Therapeutics Gwanyanya, Asfree; University of Cape Town, Human Biology
Is the invited manuscript for consideration in a Special Issue:	Not applicable (regular submission)
Keyword:	cardiac, calcium paradox, fingolimod, ion channels, TRPM7

SCHOLARONE™  
Manuscripts

**Cardioprotective effect of fingolimod against calcium paradox-induced myocardial injury in the isolated rat heart**

Fatma Alatrags, Matthew Amoni, Roisin Kelly-Laubscher, and Asfree Gwanyanya

**F. Alatrags, M. Amoni, and A. Gwanyanya.** Department of Human Biology, Faculty of Health Sciences, University of Cape Town, Observatory 7925, Cape Town, South Africa.

**R. Kelly-Laubscher.** Department of Pharmacology and Therapeutics, The College of Medicine and Health, University College Cork, Ireland.

**R. Kelly-Laubscher.** Department of Biological Sciences, Faculty of Science, University of Cape Town, Rondebosch 7700, Cape Town, South Africa.

**Corresponding author:** Asfree Gwanyanya.

Department of Human Biology, Faculty of Health Sciences, University of Cape Town, Observatory 7925, Cape Town, South Africa. Tel: +27216506400; Fax: +27214487226

*E-mail:* asfree.gwanyanya@uct.ac.za

**Abstract:** Fingolimod (FTY720) inhibits  $\text{Ca}^{2+}$ -permeable,  $\text{Mg}^{2+}$ -sensitive channels called transient receptor potential melastatin 7 (TRPM7), but its effects on  $\text{Ca}^{2+}$  paradox (CP)-induced myocardial damage have not been evaluated. We studied the effect of FTY720 on CP-induced myocardial damage, and used other TRPM7 channel inhibitors nordihydroguaiaretic acid (NDGA) and  $\text{Mg}^{2+}$  to test if any effect of FTY720 was via TRPM7 inhibition. Langendorff-perfused Wistar rat hearts were treated with FTY720 or NDGA and subjected to a CP protocol consisting of  $\text{Ca}^{2+}$  depletion followed by  $\text{Ca}^{2+}$  repletion. Hearts of rats pre-treated with  $\text{MgSO}_4$  were also subjected to CP. Hemodynamic parameters were measured using an intraventricular balloon, and myocardial infarct size was quantified using triphenyltetrazolium chloride stain. TRPM7 proteins in ventricular tissue were detected using immunoblot analysis. FTY720, but not NDGA, decreased CP-induced infarct size. Both FTY720 and NDGA minimized the CP-induced elevation of left ventricular end-diastolic pressure, but only FTY720 ultimately improved ventricular developed pressure.  $\text{Mg}^{2+}$  pre-treatment had effect neither on CP-induced infarct size, hemodynamic parameters during CP, nor the level TRPM7 protein expression in ventricular tissue. Overall, FTY720 attenuated CP-induced myocardial damage, with potential therapeutic implications on  $\text{Ca}^{2+}$ -mediated cardiotoxicity. However, the cardioprotective mechanism of FTY720 seems to be unrelated to TRPM7 channel modulation.

# **Keywords**

cardiac; calcium paradox; fingolimod; ion channels; TRPM7

## 40 Introduction

41 Abnormalities of calcium ( $\text{Ca}^{2+}$ ) homeostasis underlie the pathophysiology of life-  
42 threatening cardiovascular conditions such as myocardial injury and malignant arrhythmias  
43 (Wagner et al. 2015).  $\text{Ca}^{2+}$  paradox (CP) is a form of  $\text{Ca}^{2+}$ -mediated myocardial injury that  
44 may occur perioperatively in hearts temporarily subjected to  $\text{Ca}^{2+}$ -deficient conditions such  
45 as perfusion with  $\text{Ca}^{2+}$ -free cardioplegic solutions (Zimmerman 2000). In other non-  
46 perioperative situations, cardiac  $\text{Ca}^{2+}$  paradox could occur in a subtle form and remain  
47 relatively undetected in conditions of temporary  $\text{Ca}^{2+}$  deficits. Unlike the myocardium  
48 damage due to ischemia/reperfusion injury, CP can occur even with continuous tissue  
49 perfusion (Mani et al. 2015, Piper 2000). During CP, the removal of extracellular  $\text{Ca}^{2+}$   
50 induces cardiac intracellular- and intercellular molecular changes that make cardiomyocytes  
51 susceptible to damage upon the re-introduction of extracellular  $\text{Ca}^{2+}$  ions (Aggeli et al. 2013,  
52 Hearse et al. 1978, Zimmerman 2000). Unfortunately, preventative options for CP remain  
53 limited because the underlying mechanisms are not fully understood. The known  
54 abnormalities in CP include myocardial ultra-structural damage mainly due to  $\text{Ca}^{2+}$  overload  
55 as well as due to cell-cell separation and ATP depletion, even in the absence of ischemia  
56 (Kovacs et al. 2017, Mani et al. 2015, Piper 2000). The  $\text{Ca}^{2+}$  overload in CP may occur via  
57  $\text{Ca}^{2+}$ -selective channels such as L-type  $\text{Ca}^{2+}$  channels or secondary to  $\text{Na}^{+}$  overload via the  
58 action of the reverse-mode  $\text{Na}^{+}/\text{Ca}^{2+}$  exchanger (Guppy et al. 1999, Karmazyn et al. 1993,  
59 Piper 2000). It has also been suggested to occur via  $\text{Ca}^{2+}$ -permeable channels such as  
60 transient receptor potential (TRP) channels (Bosteels et al. 1999, Kojima et al. 2010).

61 Fingolimod (FTY720) is a drug used in the treatment of multiple sclerosis, but some  
62 studies have also demonstrated its ability to protect against cardiovascular conditions such as  
63 ischemia/reperfusion myocardial injury (Hofmann et al. 2009, Santos-Gallego et al. 2016,  
64 Vessey et al. 2013) and arrhythmias (Egom et al. 2010, Egom et al. 2015). Nonetheless, even

in the context of ischemia/reperfusion injury, the effect of FTY720 is still not fully known since both pro-arrhythmic and anti-arrhythmic effects of FTY720 have been observed in the same disease model, depending on the timing of drug administration (Hofmann et al. 2010). Furthermore, in ischemia/reperfusion injury models, FTY720 has been shown either to reduce infarct size (van Vuuren et al. 2016), to have no effect on infarct size, despite hemodynamic improvements (Hofmann et al. 2009, Hofmann et al. 2010), or to have a dose-dependent differential effect on functional recovery (van Vuuren et al. 2016).

The pathophysiological mechanisms of disease conditions such as ischemia/reperfusion myocardial injury are distinctly different from that of CP (Piper 2000), and as such the effect of FTY720 on CP-induced myocardial damage is unknown. FTY720 is a sphingosine analogue. When protecting the heart against damage caused by ischemia/reperfusion injury or arrhythmias, FTY720 has been shown to act through S1P receptor-dependent mechanisms and activation of pro-survival kinases to protect the heart (Ahmed et al. 2019, Egom et al. 2010, Hofmann et al. 2009, Hofmann et al. 2010, Santos-Gallego et al. 2016). Interestingly, FTY720 also acts via S1P receptor-independent pathways to protect the heart (Vessey et al. 2013). One of these mechanisms is via its inhibition of the enzyme S1P lyase (Bandhuvula et al. 2005), the inhibition of which is linked to the cardioprotection against ischemia/reperfusion injury (Bandhuvula et al. 2011). However, FTY720 can also inhibit the  $Mg^{2+}$ -sensitive,  $Ca^{2+}$ -permeable TRP melastatin 7 (TRPM7) channels (Qin et al. 2013). The TRPM7 channels mediate cellular entry of  $Ca^{2+}$  and other divalent cations (Gwanyanya et al. 2004, Monteilh-Zoller et al. 2003, Nadler et al. 2001). Considering the major changes in  $Ca^{2+}$  homeostasis that occur in several cardiac pathologies, it is possible that FTY720 may also protect the heart via its modulation of these channels.

In this study, we therefore investigated the effect of FTY720 on CP-induced myocardial damage. We also tested whether FTY720 may act via inhibiting TRPM7 channels

90 by using another chemically-unrelated TRPM7 inhibitor nordihydroguaiaretic acid (NDGA)  
91 (Chen et al. 2010) as well as  $Mg^{2+}$ , given its intracellular inhibition of TRPM7 channels  
92 (Gwanyanya et al. 2004, Monteilh-Zoller et al. 2003). TRPM7 channels were targeted  
93 because they are a relatively new type of  $Ca^{2+}$ -permeable channels that are known to be  
94 inhibited by fingolimod, and therefore can become therapeutic drug targets. As for  $Mg^{2+}$ , its  
95 extracellular application is already known to protect against  $Ca^{2+}$  paradox in guinea pig hearts  
96 (Suleiman et al. 1993), so we tested for a different, intracellular effect of  $Mg^{2+}$  on CP via  
97 TRPM7 inhibition.

Draft

## 98 **Materials and methods**

### 99 **Animals**

100 The study was approved by the Faculty of Health Sciences Animal Research Ethics  
101 Committee of the University of Cape Town (AEC Protocol 014-014), and all research  
102 involving animals was conducted according to the Canadian Council on Animal Care  
103 (CCAC) guidelines and the Guide for the Care and Use of Laboratory Animals (8th edition,  
104 National Academies Press). Adult male Wistar rats (250–300 g) were housed under  
105 standardized conditions (12-hour light/dark cycle and temperature of 23°C) and had  
106 unlimited access to rat chow and drinking water. Rats used to test  $Mg^{2+}$  effects were injected  
107 intraperitoneally (i.p.) with either  $MgSO_4$  (270 mg/kg) or an equivalent volume of saline  
108 daily for 7 consecutive days (Amoni et al. 2017b, Sameshima et al. 1999). The  $MgSO_4$  salt  
109 was chosen as it is more often clinically used than say  $MgCl_2$  (Durlach et al. 2005), and also  
110 offsets any enteral-route related toxicity when administered intraperitoneally as was done in  
111 this study. For enteral administration,  $MgCl_2$  would have been a better choice, given its lower  
112 enteral toxicity profile (Durlach et al. 2005). In addition, the  $MgSO_4$  pharmacokinetic profile  
113 in rats has been determined in other tissue-protection studies (Sameshima et al. 1999).  $Mg^{2+}$   
114 was administered as pre-treatment in vivo, rather than acutely on isolated hearts in order to  
115 allow the  $Mg^{2+}$  to enter cells and exert its TRPM7 channel inhibitory effects from the  
116 intracellular compartment (Gwanyanya et al. 2004, Monteilh-Zoller et al. 2003, Nadler et al.  
117 2001). The experiments on  $Mg^{2+}$ -treated rats were performed 24 hours after the final  $MgSO_4$   
118 or saline injection to exclude direct extracellular effects of  $Mg^{2+}$ .

119

### 120 **Heart isolation and perfusion protocols**



121 Unless stated otherwise, chemicals were obtained from Sigma (Sigma-Aldrich, SA).  
122 Hearts were removed for Langendorff perfusion as previously described (Araibi et al. 2020).  
123 Briefly, rats were anticoagulated with heparin (500 I.U./kg, i.p.) and anesthetized with  
124 sodium pentobarbital (70 mg/kg i.p., Vertserv, SA). Hearts were rapidly removed and placed  
125 in cold (4°C), filtered (Whatman filter paper, Sigma-Aldrich, SA), modified Krebs-Henseleit  
126 (K-H) solution containing (in mmol/L): 118.5 NaCl, 4.7 KCl, 25 NaHCO<sub>3</sub>, 1.2 MgSO<sub>4</sub>,  
127 1.8 CaCl<sub>2</sub>, 1.2 KH<sub>2</sub>PO<sub>4</sub> and 11 glucose; pH 7.4, gassed with 95%O<sub>2</sub> and 5%CO<sub>2</sub>). For  
128 perfusion studies, the aorta was cannulated for retrograde perfusion with K-H solution  
129 (maintained at 37°C) on a constant-pressure (74 mmHg) Langendorff perfusion apparatus  
130 (Fig. 1A). To induce Ca<sup>2+</sup> paradox, a parallel Langendorff apparatus was used to deliver  
131 Ca<sup>2+</sup>-free K-H solution, and this system converged with the main perfusion system via a 3-  
132 way stop cock positioned above the aortic cannula (Fig. 1A). The Ca<sup>2+</sup>-free K-H solution was  
133 made by excluding CaCl<sub>2</sub> from K-H solution and adding 0.5 mmol/L EGTA.

134 Hearts used to test the effects of fingolimod (FTY720) and NDGA were randomly  
135 assigned to 6 groups (Fig. 1B), whereas those used to test the effect of Mg<sup>2+</sup> were assigned to  
136 4 groups (Fig. 4A), with each group named according to the perfusion- and drug  
137 administration protocol used. Hearts were stabilized on the perfusion system for 20 minutes  
138 prior to drug treatments. The CP protocol consisted of heart perfusion with Ca<sup>2+</sup>-free K-H  
139 solution for 3 minutes, followed by the re-introduction of Ca<sup>2+</sup>-containing solution for 30  
140 minutes (Bi et al. 2012). FTY720 (1 µmol/L) and NDGA (10 µmol/L) were dissolved in  
141 DMSO (final concentration < 0.01%) and administered for 5 minutes before the  
142 commencement of the CP protocol. The concentrations of these drugs used are adequate to  
143 inhibit TRPM7 channels (Chen et al. 2010, Qin et al. 2013). The drugs were delivered into  
144 the perfusate column through a 3-way stop cock using a syringe pump (Graseby 2100, Smith  
145 Medical, SA; Fig 1A) set to run at 10% of the coronary flow rate in order to minimize

disturbances in perfusion pressure. The concentration of the drug in the syringe was 10 times higher than the final concentration to cater for the dilution by the main perfusion column. The coronary flow rate was measured by timed collection of coronary effluent. At the end of perfusion, hearts were stored at -20°C for infarct size measurements.

### **Hemodynamic parameter measurements**

Left ventricular (LV) pressure was measured using a water-filled, intraventricular balloon (Fig. 1A) mounted at the tip of a catheter connected to a blood pressure transducer (MLT1199) and amplifier (Bridge Amp ML221, ADInstruments, Australia). The balloon was inflated to a LV end-diastolic pressure (LVEDP) of 5–10 mmHg, and the balloon volume was not altered thereafter. Hemodynamic parameters were recorded using the PowerLab data-acquisition system and LabChart 7 software (ADInstruments, Australia) and were analyzed using the LabChart 7 Pro BP module (ADInstruments, Australia). The LV developed pressure (LVDP) was obtained as the difference between peak systolic pressure and LVEDP.

### **Infarct size measurements**

Ventricles of frozen hearts were cut transversely into a series of 2-mm slices from apex to base and thawed for 2,3,5-triphenyltetrazolium chloride (TTC) staining as previously described (Amoni et al. 2017b, Araibi et al. 2020). Infarct size was measured as TTC-negative area on the slices from each heart using ImageJ software (NIH, USA) and was expressed as a percentage of the total ventricular area (Araibi et al. 2020).

### **Western immunoblotting**

Western blot analysis was performed as previously described (Aboalgasm et al. 2021a, Aboalgasm et al. 2021b). Sections of frozen LV tissue (approximately 0.05 g) were

171 homogenized on ice by sonication in a modified radioimmunoprecipitation assay (RIPA)  
172 lysis buffer (50 mM Tris-HCl, 150 mM NaCl, 1% Triton X-100, 0.5% sodium deoxycholate,  
173 0.1% sodium dodecyl sulphate, pH 7.4) containing a protease/phosphatase inhibitor cocktail  
174 (HALT, Thermo Fisher Scientific, Rockford, USA). The samples were mixed on a vortex and  
175 centrifuged at 15 000 g for 30 minutes at 4°C. The supernatant was decanted, and the protein  
176 concentration was quantified using a BCA protein assay kit (Thermo Fisher Scientific,  
177 Rockford, USA). Lysates were denatured at 95°C for 5 minutes in a mixture of Laemmli  
178 buffer (Bio-Rad, SA), RIPA buffer, and diethyltritol. Protein samples (40 µg) were  
179 electrophoresed on 12% SDS-PAGE gels using a Mini-PROTEAN Tetra Cell system  
180 (Bio-Rad, SA) and transferred to nitrocellulose membrane using a Trans-Blot turbo transfer  
181 system (Bio-Rad, SA). Gel electrophoresis and protein transfer to membrane were confirmed  
182 by Ponceau S staining. The membrane was blocked with 5% milk in 0.1% Tween-20  
183 phosphate-buffered saline (PBS-T) at 4°C for 3 hours, and incubated with anti-TRPM7  
184 mouse monoclonal primary antibody (1:8000, Abcam 85016, USA) in 5% milk PBS-T  
185 overnight at 4°C. In the negative control, anti-TRPM7 antibody was excluded to rule out non-  
186 specific binding of secondary antibody. The membrane was then washed in PBS-T and  
187 incubated with horseradish peroxidase-linked goat anti-mouse secondary antibody (1:20 000,  
188 Abcam 205719, USA) in 5% milk PBS-T for 1 hour at room temperature. Blots were  
189 developed by adding an enhanced chemiluminescence substrate (Bio-Rad, SA) and exposure  
190 to X-ray film. The film images were scanned and analysed using ImageJ software (NIH,  
191 USA). The membrane was thereafter washed in water, stripped with 8% NaOH, blocked for 3  
192 hours with 5% BSA in PBS-T, and re-probed with anti-β-actin mouse monoclonal primary  
193 antibody (1:15000, Abcam 8226, USA) and goat anti-mouse secondary antibody (1:20 000,  
194 Abcam 205719, USA).

195

## 196 **Plasma Mg<sup>2+</sup> measurements**

197           Blood used for Mg<sup>2+</sup> measurements was collected at the time of excision of the heart  
198 (24 hours after the final MgSO<sub>4</sub> or saline injection). The blood was centrifuged to obtain  
199 plasma, from which ionized Mg<sup>2+</sup> concentration was measured using photometric assays  
200 (Beckman AU, PathCare, SA) as previously described (Amoni et al. 2017a).

201

## 202 **Data analysis**

203           Data are expressed as mean and standard error of mean (SEM), with *n* indicating the  
204 number of rats studied under each condition. Statistical analysis was conducted using  
205 Statistica (v.13). Differences among multiple groups were evaluated using analysis of  
206 variance (ANOVA) and Tukey's *post-hoc* test or repeated-measures ANOVA. Differences  
207 between two independent groups were compared using unpaired *t*-test. *P* < 0.05 was  
208 considered statistically significant.

## 209   **Results**

### 210   **Effects of FTY720 and NDGA on CP-induced infarct size**

211           Representative images of TTC-stained ventricular slices (Fig. 2A) show a  
212   prominent TTC-negative ventricular area in the CP heart compared to that in the control  
213   heart, which is indicative of CP-induced myocardial damage. The application of FTY720  
214   (1  $\mu\text{mol/L}$ ), but not NDGA (10  $\mu\text{mol/L}$ ), significantly decreased CP-induced infarct size from  
215    $64.6 \pm 5.3\%$  to  $39.0 \pm 6.8\%$  ( $P = 0.001$ ; Fig. 2B). The sizes of background infarcts due to  
216   handling artefacts in non-CP hearts (i.e., control and drug only treated hearts) were not  
217   significantly different from each other ( $P = 0.78$ ) but were significantly smaller than the  
218   infarcts in CP hearts ( $P < 0.001$ ; Fig. 2B).

### 220   **Effects of FTY720 and NDGA on CP-induced hemodynamic parameters**

221           A typical CP protocol (Fig. 3A) produced a complete loss of ventricular force of  
222   contraction and an elevation of LVEDP during the periods of  $\text{Ca}^{2+}$  depletion and  $\text{Ca}^{2+}$   
223   repletion (LVEDP:  $P < 0.001$  for CP vs. control; Fig. 3B), whereas the ventricular force of  
224   contraction and LVEDP in control, non-CP hearts remained relatively stable over the  
225   duration of perfusion. Although there was still an elevation of LVEDP due to CP, both  
226   FTY720 and NDGA decreased the extent of CP-induced elevation of LVEDP compared to  
227   CP alone ( $P = 0.039$  for FTY720 + CP vs. CP and  $P = 0.020$  for NDGA + CP vs. CP;  
228   Fig. 3B). However, only FTY720 significantly improved LVDP during CP ( $P = 0.029$ ,  
229   FTY720 + CP vs. CP; Fig. 3C). In the absence of CP, neither FTY720 nor NDGA altered  
230   LVDP compared to control ( $P = 0.90$ ; Fig. 3C). However, FTY720 alone increased LVEDP  
231   in the absence of CP compared to control ( $P = 0.003$ ), but this increase was still significantly  
232   lower than the LVEDP in CP (Fig. 3B). Neither CP nor the application of drugs (FTY720 or

NDGA) had statistically significant effect on coronary flow rate compared to control ( $P = 0.40$ ; Fig. 3D).

### **Effect of $Mg^{2+}$ on CP**

We also tested effects of  $Mg^{2+}$  as an additional type of TRPM7 channel inhibitor. This ion has a different inhibitory action since it acts intracellularly as compared to the extracellular effects of FTY720 and NDGA.  $Mg^{2+}$  pre-treatment did not significantly alter CP-induced infarct size ( $50.7 \pm 3.7\%$  for CP vs.  $50.2 \pm 4.1\%$  for  $Mg^{2+}$  + CP,  $P = 0.98$ ; Fig. 4B and Fig. 4C). The sizes of background infarcts in non-CP hearts were not significantly different from each other (infarct size:  $7.4 \pm 0.5\%$  for control vs.  $6.4 \pm 0.5\%$  for  $Mg^{2+}$  pre-treated,  $P = 0.90$ ), but were significantly smaller than the infarcts in CP hearts ( $P < 0.001$ , CP vs. control or  $Mg^{2+}$ ; Fig. 4B and Fig. 4C).  $Mg^{2+}$  pre-treatment also did not reverse the CP-induced changes in LVEDP or LVDP (Fig. 4D and Fig. 4E). In the absence of CP, pre-treatment with  $Mg^{2+}$  had no significant effect on LVDP or LVEDP (Fig. 4D and Fig. 4E). Furthermore,  $Mg^{2+}$  concentration was measured to verify plasma normomagnesemia at the time of CP experiments. The plasma  $Mg^{2+}$  concentration was not significantly different between  $Mg^{2+}$  pre-treated rats and controls ( $0.87 \pm 0.03$  mmol/L for control vs.  $0.93 \pm 0.04$  mmol/L for  $Mg^{2+}$  pre-treated;  $P = 0.62$ ,  $n = 5$  rats per group).

### **TRPM7 immunoblotting**

In order to verify the presence of TRPM7 channels and the possible modulation by  $Mg^{2+}$  pre-treatment in the rat hearts used in our experiments, TRPM7 immunoblotting was performed in ventricular tissue. Images of western blot analysis (Fig. 5A) showed the immune-detection of both TRPM7- and the loading control  $\beta$ -actin proteins in cardiac LV tissue. In contrast, the TRPM7 signal was virtually undetectable in the negative controls in

258 which the anti-TRPM7 primary antibody was omitted ( $P = 0.003$  vs. TRPM7;  $n = 6$  rats per  
259 group; result not illustrated). The intensity of the TRPM7 bands on films appeared similar in  
260 ventricular tissue of control rats and  $Mg^{2+}$  pre-treated rats (Fig. 5A). As such, there was no  
261 statistically significant difference in the level of TRPM7 protein expression between  
262 ventricular tissue of control- and  $Mg^{2+}$  pre-treated rats ( $P = 0.43$ ; Fig. 5B).

Draft

## Discussion

CP represents a unique,  $\text{Ca}^{2+}$ -related threat to perioperative cardiovascular tissue survival, even in the absence of ischemia (Piper 2000, Zimmerman 2000). The results of the present study showed that FTY720, but not NDGA nor  $\text{Mg}^{2+}$ , decreased CP-induced infarct size and improved LV functional recovery.

In this study, FTY720 was partially effective at rescuing contractile function of the heart during CP as was evidenced by improved LVDP; minimized cardiac tissue death from CP-induced myocardial injury as was evidenced by the reduction in infarct size; and reduced the extent of dysfunctional contractures as was indicated by decreased LVEDP during CP. Although some studies have demonstrated cardioprotective effects of FTY720 in models of ischemia/reperfusion injury and cardiac arrhythmia, this cardioprotective effect of FTY720 during CP seems to be a novel finding since there were no previous reports that we could find that specifically addressed the effect of FTY720 on CP. However, we also noticed that FTY720, on its own, increased LVEDP by the end of perfusion compared to control hearts. The reason for this increase was not clear, but other studies showed that the infusion of FTY720 in conscious rodents increased mean arterial pressure (Forrest et al. 2004), and that FTY720, when orally administered, induced hypertension in rodents (Fryer et al. 2012). In contrast, in healthy human subjects, FTY720 induced transient decreases in mean arterial pressure (Schmouder et al. 2006). Such effects of FTY720 on blood pressure as well as the induction of bradycardia (Faber et al. 2013) therefore constitute important side effects to be recognized in the utility of the drug in cardioprotection. Nonetheless, the increase in LVEDP by FTY720 observed in the present study did not undermine the overall improvement of LVDP during CP.

The mechanism underlying the cardioprotective effect of FTY720 during CP is unclear since the inhibition of TRPM7 channel did not seem to mediate the effect. In our



study, there was a lack of cardioprotection against CP by NDGA, a chemical which, similar to FTY720, inhibits the  $\text{Ca}^{2+}$ -permeable TRPM7 channels at the doses administered (Chen et al. 2010, Qin et al. 2013). The lack of NDGA effect was despite the presence of TRPM7 protein in the rat hearts used in our experiments as was confirmed by the positive TRPM7 immunoblots in LV tissue. Consistent with the findings from another study (Murphy et al. 1995), in our study, NDGA, on its own, had no detrimental effects on cardiac hemodynamic function, but rather stabilized LVEDP during CP. However, NDGA was also shown to impair protective effects of cardiac preconditioning via the lipoxygenase pathway (Murphy et al. 1995) but such a mechanism may not be relevant to CP since the inhibition of TRPM7 channels by NDGA is lipoxygenase-independent (Chen et al. 2010). Furthermore, in our study,  $\text{Mg}^{2+}$  pre-treatment did not alter CP, suggesting that the intracellular inhibitory effect of  $\text{Mg}^{2+}$  on TRPM7 channels did not modulate CP. The protective effect of acute extracellular  $\text{Mg}^{2+}$  against CP observed in guinea pig hearts (Suleiman et al. 1993) is different from an intracellular inhibition of TRPM7 channels, and therefore would not be applicable in the present study since the plasma  $\text{Mg}^{2+}$  concentration had reverted to normal at the time of CP experiments as was verified by  $\text{Mg}^{2+}$  assays. Taken together, our results suggest that the cardioprotective effect of FTY720 during CP may be unrelated to the inhibition of TRPM7 channels. The possible contribution to CP of other TRP channels that belong to the same melastatin subfamily as TRPM7 channels such as TRPM4 is not known. TRPM4 channels are highly selective for monovalent cations such as  $\text{Na}^+$  (Launay et al. 2002), and it has been proposed that the monovalent cation influx through them could induce membrane depolarisation that may, in turn, cause  $\text{Ca}^{2+}$  influx via  $\text{Ca}^{2+}$ -permeable channels, thereby modulating cardiac activity (Alonso-Carbajo et al. 2017). However, there is no evidence yet to support this possibility for  $\text{Ca}^{2+}$  influx through TRPM7 channels, which would otherwise be relevant in CP. In addition, such an effect would most likely affect voltage-gated  $\text{Ca}^{2+}$ -

permeable channels, rather than TRPM7 channels, for which the gating is voltage-independent (Gwanyanya et al. 2004, Monteilh-Zoller et al. 2003, Nadler et al. 2001).

Most of what is currently known about the cardiac effects of FTY720 relates to the models of ischemia/reperfusion injury. Although  $\text{Ca}^{2+}$  dysregulation may be involved in both ischemia/reperfusion injury and  $\text{Ca}^{2+}$  paradox, these conditions are different.  $\text{Ca}^{2+}$  paradox is not often easily recognised as it presents with some features similar to those of ischemia/reperfusion injury (Hearse et al. 1978), yet it is a detrimental clinical entity that occurs even in the absence of an ischemic insult (Aggeli et al. 2013, Hearse et al. 1978, Zimmerman 2000). Furthermore, given that  $\text{Ca}^{2+}$  paradox represents a complication of temporary  $\text{Ca}^{2+}$  deficit, but, at the same time,  $\text{Ca}^{2+}$  abnormalities are known to affect a plethora of cellular functions, its manifestation could be missed and attributed to other well-known  $\text{Ca}^{2+}$ -related cellular events. However, an important limitation in studying  $\text{Ca}^{2+}$  paradox (as was done in the present study) is that the standard experimental protocol of extracellular  $\text{Ca}^{2+}$  exclusion is extreme and unphysiological, but at the same time, it has the advantage that it amplifies and quickens the subtle tissue damage that would otherwise occur undetected whenever there is a temporary  $\text{Ca}^{2+}$  deficit (Piper 2000). Our results, therefore, show the potential of FTY720 as a cardioprotective agent against  $\text{Ca}^{2+}$  paradox, a novelty that has not been described in  $\text{Ca}^{2+}$  paradox. This FTY720 effect on CP is therefore different from the FTY720 modulation of other cardiac conditions such as ischaemia/reperfusion injury. However, the exact mechanism underlying the protective effect of FTY720 against CP was not established in the present study.

In conclusion, the results of this study showed that FTY720, but not NDGA or  $\text{Mg}^{2+}$ , partially reduced CP-induced myocardial damage and improved cardiac contractile function. Clinically, given that FTY720 is already being used in the treatment of multiple sclerosis, this cardioprotective effect may represent a novel therapeutic role of the drug (or in combination

338 with other protective drugs) in attenuating CP-induced myocardial damage during  
339 perioperative cardiac perfusion. The results suggest that the cardioprotective action of  
340 FTY720 during CP may be unrelated to the inhibition of TRPM7 channels, but the exact  
341 underlying mechanism still requires further investigation.

Draft

## 342 **Acknowledgements**

343           This work was supported by the South African Medical Research Council (MRC  
344   SIR Grant number 29841) and the National Research Foundation South Africa (NRF  
345   Grant numbers 85768 and 91514). **Conflict of interest:** The authors declare no conflict  
346   of interest.

Draft

**References**

- Aboalgasm, H., Ballo, R., Mkatazo, T. & Gwanyanya, A. 2021a. Hyperglycaemia-Induced Contractile Dysfunction and Apoptosis in Cardiomyocyte-Like Pulsatile Cells Derived from Mouse Embryonic Stem Cells. *Cardiovasc Toxicol.* **21**(9): 695-709. doi:10.1007/s12012-021-09660-3. PMID:33983555.
- Aboalgasm, H., Petersen, M. & Gwanyanya, A. 2021b. Improvement of cardiac ventricular function by magnesium treatment in chronic streptozotocin-induced diabetic rat heart. *Cardiovasc J Afr.* **32**(3): 141-148. doi:10.5830/CVJA-2020-054. PMID:33300932.
- Aggeli, I.K., Zacharias, T., Papapavlou, G., Gaitanaki, C. & Beis, I. 2013. Calcium paradox induces apoptosis in the isolated perfused *Rana ridibunda* heart: involvement of p38-MAPK and calpain. *Can J Physiol Pharmacol.* **91**(12): 1095-1106. doi:10.1139/cjpp-2013-0081. PMID:24289081.
- Ahmed, N., Mehmood, A., Linardi, D., Sadiq, S., Tessari, M., Meo, S.A., Rehman, R., Hajjar, W.M., et al. 2019. Cardioprotective Effects of Sphingosine-1-Phosphate Receptor Immunomodulator FTY720 in a Clinically Relevant Model of Cardioplegic Arrest and Cardiopulmonary Bypass. *Front. Pharmacol.* **10**: 802. doi:10.3389/fphar.2019.00802. PMID:31379576.
- Alonso-Carbajo, L., Kecskes, M., Jacobs, G., Pironet, A., Syam, N., Talavera, K. & Vennekens, R. 2017. Muscling in on TRP channels in vascular smooth muscle cells and cardiomyocytes. *Cell Calcium.* **66**: 48-61. doi:10.1016/j.ceca.2017.06.004. PMID:28807149.
- Amoni, M., Kelly-Laubscher, R., Blackhurst, D. & Gwanyanya, A. 2017a. Beneficial Effects of Magnesium Treatment on Heart Rate Variability and Cardiac Ventricular Function in Diabetic Rats. *J Cardiovasc Pharmacol Ther.* **22**(2): 169-178. doi:10.1177/1074248416653831. PMID:27276916.

- 372 Amoni, M., Kelly-Laubscher, R., Petersen, M. & Gwanyanya, A. 2017b. Cardioprotective  
373 and Anti-arrhythmic Effects of Magnesium Pretreatment Against  
374 Ischaemia/Reperfusion Injury in Isoprenaline-Induced Hypertrophic Rat Heart.  
375 Cardiovasc Toxicol. **17**(1): 49-57. doi:10.1007/s12012-015-9355-6. PMID:26696240.
- 376 Araibi, H., Van Der Merwe, E., Gwanyanya, A. & Kelly-Laubscher, R. 2020. The effect of  
377 sphingosine-1-phosphate on the endothelial glycocalyx during ischemia-reperfusion  
378 injury in the isolated rat heart. Microcirculation. **27**(5): e12612.  
379 doi:10.1111/micc.12612. PMID:32017300.
- 380 Bandhuvula, P., Honbo, N., Wang, G.Y., Jin, Z.Q., Fyrist, H., Zhang, M., Borowsky, A.D.,  
381 Dillard, L., et al. 2011. S1P lyase: a novel therapeutic target for ischemia-reperfusion  
382 injury of the heart. Am J Physiol Heart Circ Physiol. **300**(5): H1753-1761.  
383 doi:10.1152/ajpheart.00946.2010. PMID:21335477.
- 384 Bandhuvula, P., Tam, Y.Y., Oskouian, B. & Saba, J.D. 2005. The immune modulator  
385 FTY720 inhibits sphingosine-1-phosphate lyase activity. J. Biol. Chem. **280**(40):  
386 33697-33700. doi:10.1074/jbc.C500294200. PMID:16118221.
- 387 Bi, S.H., Jin, Z.X., Zhang, J.Y., Chen, T., Zhang, S.L., Yang, Y., Duan, W.X., Yi, D.H., et al.  
388 2012. Calpain inhibitor MDL 28170 protects against the Ca<sup>2+</sup> paradox in rat hearts. Clin  
389 Exp Pharmacol Physiol. **39**(4): 385-392. doi:10.1111/j.1440-1681.2012.05683.x.  
390 PMID:22356295.
- 391 Bosteels, S., Matejovic, P., Flameng, W. & Mubagwa, K. 1999. Sodium influx via a non-  
392 selective pathway activated by the removal of extracellular divalent cations: possible  
393 role in the calcium paradox. Cardiovasc Res. **43**(2): 417-425. doi:10.1016/s0008-  
394 6363(99)00098-x. PMID:10536672.

- 395 Chen, H.C., Xie, J., Zhang, Z., Su, L.T., Yue, L. & Runnels, L.W. 2010. Blockade of TRPM7  
396 channel activity and cell death by inhibitors of 5-lipoxygenase. *PLoS One*. **5**(6):  
397 e11161. doi:10.1371/journal.pone.0011161. PMID:20567598.
- 398 Durlach, J., Guiet-Bara, A., Pages, N., Bac, P. & Bara, M. 2005. Magnesium chloride or  
399 magnesium sulfate: a genuine question. *Magnes. Res.* **18**(3): 187-192. PMID:16259379.
- 400 Egom, E.E., Ke, Y., Musa, H., Mohamed, T.M., Wang, T., Cartwright, E., Solaro, R.J. & Lei,  
401 M. 2010. FTY720 prevents ischemia/reperfusion injury-associated arrhythmias in an ex  
402 vivo rat heart model via activation of Pak1/Akt signaling. *J. Mol. Cell. Cardiol.* **48**(2):  
403 406-414. doi:10.1016/j.yjmcc.2009.10.009. PMID:19852968.
- 404 Egom, E.E., Kruzliak, P., Rotrekl, V. & Lei, M. 2015. The effect of the sphingosine-1-  
405 phosphate analogue FTY720 on atrioventricular nodal tissue. *J Cell Mol Med.* **19**(7):  
406 1729-1734. doi:10.1111/jcmm.12549. PMID:25864579.
- 407 Faber, H., Fischer, H.J. & Weber, F. 2013. Prolonged and symptomatic bradycardia  
408 following a single dose of fingolimod. *Mult. Scler.* **19**(1): 126-128.  
409 doi:10.1177/1352458512447596. PMID:22729989.
- 410 Forrest, M., Sun, S.Y., Hajdu, R., Bergstrom, J., Card, D., Doherty, G., Hale, J., Keohane, C.,  
411 et al. 2004. Immune cell regulation and cardiovascular effects of sphingosine 1-  
412 phosphate receptor agonists in rodents are mediated via distinct receptor subtypes. *J*  
413 *Pharmacol Exp Ther.* **309**(2): 758-768. doi:10.1124/jpet.103.062828. PMID:14747617.
- 414 Fryer, R.M., Muthukumarana, A., Harrison, P.C., Nodop Mazurek, S., Chen, R.R.,  
415 Harrington, K.E., Dinallo, R.M., Horan, J.C., et al. 2012. The clinically-tested S1P  
416 receptor agonists, FTY720 and BAF312, demonstrate subtype-specific bradycardia  
417 (S1P(1)) and hypertension (S1P(3)) in rat. *PLoS One*. **7**(12): e52985.  
418 doi:10.1371/journal.pone.0052985. PMID:23285242.

- 419 Guppy, L.J. & Littleton, J.M. 1999. Damaging effects of the calcium paradox are reduced in  
420 isolated hearts from ethanol-dependent rats: paradoxical effects of dihydropyridine drugs.  
421 J. Cardiovasc. Pharmacol. **34**(6): 765-771. doi:10.1097/00005344-199912000-00001.  
422 PMID:10598118.
- 423 Gwanyanya, A., Amuzescu, B., Zakharov, S.I., Macianskiene, R., Sipido, K.R., Bolotina,  
424 V.M., Vereecke, J. & Mubagwa, K. 2004. Magnesium-inhibited, TRPM6/7-like  
425 channel in cardiac myocytes: permeation of divalent cations and pH-mediated  
426 regulation. J Physiol. **559**(Pt 3): 761-776. doi:10.1113/jphysiol.2004.067637.  
427 PMID:15272039.
- 428 Hearse, D.J., Humphrey, S.M., Boink, A.B. & Ruigrok, T.J. 1978. The calcium paradox:  
429 metabolic, electrophysiological, contractile and ultrastructural characteristics in four  
430 species. Eur. J. Cardiol. **7**(4): 241-256. PMID:689059.
- 431 Hofmann, U., Burkard, N., Vogt, C., Thoma, A., Frantz, S., Ertl, G., Ritter, O. & Bonz, A.  
432 2009. Protective effects of sphingosine-1-phosphate receptor agonist treatment after  
433 myocardial ischaemia-reperfusion. Cardiovasc Res. **83**(2): 285-293.  
434 doi:10.1093/cvr/cvp137. PMID:19416991.
- 435 Hofmann, U., Hu, K., Walter, F., Burkard, N., Ertl, G., Bauersachs, J., Ritter, O., Frantz, S.,  
436 et al. 2010. Pharmacological pre- and post-conditioning with the sphingosine-1-  
437 phosphate receptor modulator FTY720 after myocardial ischaemia-reperfusion. Br J  
438 Pharmacol. **160**(5): 1243-1251. doi:10.1111/j.1476-5381.2010.00767.x.  
439 PMID:20590616.
- 440 Karmazyn, M., Ray, M. & Haist, J.V. 1993. Comparative effects of Na<sup>+</sup>/H<sup>+</sup> exchange  
441 inhibitors against cardiac injury produced by ischemia/reperfusion,  
442 hypoxia/reoxygenation, and the calcium paradox. J. Cardiovasc. Pharmacol. **21**(1): 172-  
443 178. doi:10.1097/00005344-199301000-00025. PMID:7678674.



- 444 Kojima, A., Kitagawa, H., Omatsu-Kanbe, M., Matsuura, H. & Nosaka, S. 2010.  $\text{Ca}^{2+}$   
445 paradox injury mediated through TRPC channels in mouse ventricular myocytes. *Br J*  
446 *Pharmacol.* **161**(8): 1734-1750. doi:10.1111/j.1476-5381.2010.00986.x.  
447 PMID:20718730.
- 448 Kovacs, A., Kalasz, J., Pasztor, E.T., Toth, A., Papp, Z., Dhalla, N.S. & Barta, J. 2017.  
449 Myosin heavy chain and cardiac troponin T damage is associated with impaired  
450 myofibrillar ATPase activity contributing to sarcomeric dysfunction in  $\text{Ca}^{2+}$ -paradox rat  
451 hearts. *Mol Cell Biochem.* **430**(1-2): 57-68. doi:10.1007/s11010-017-2954-8.  
452 PMID:28213770.
- 453 Launay, P., Fleig, A., Perraud, A.L., Scharenberg, A.M., Penner, R. & Kinet, J.P. 2002.  
454 TRPM4 is a  $\text{Ca}^{2+}$ -activated nonselective cation channel mediating cell membrane  
455 depolarization. *Cell.* **109**(3): 397-407. doi:10.1016/s0092-8674(02)00719-5.  
456 PMID:12015988.
- 457 Mani, H., Tanaka, H., Adachi, T., Ikegawa, M., Dai, P., Fujita, N. & Takamatsu, T. 2015.  
458 How Does the  $\text{Ca}^{2+}$ -paradox Injury Induce Contracture in the Heart? - A Combined  
459 Study of the Intracellular  $\text{Ca}^{2+}$  Dynamics and Cell Structures in Perfused Rat Hearts.  
460 *Acta Histochem. Cytochem.* **48**(1): 1-8. doi:10.1267/ahc.14059. PMID:25861132.
- 461 Monteilh-Zoller, M.K., Hermosura, M.C., Nadler, M.J., Scharenberg, A.M., Penner, R. &  
462 Fleig, A. 2003. TRPM7 provides an ion channel mechanism for cellular entry of trace  
463 metal ions. *J. Gen. Physiol.* **121**(1): 49-60. doi:10.1085/jgp.20028740.  
464 PMID:12508053.
- 465 Murphy, E., Glasgow, W., Fralix, T. & Steenbergen, C. 1995. Role of lipoxygenase  
466 metabolites in ischemic preconditioning. *Circ Res.* **76**(3): 457-467.  
467 doi:10.1161/01.res.76.3.457. PMID:7859391.

- 468 Nadler, M.J., Hermosura, M.C., Inabe, K., Perraud, A.L., Zhu, Q., Stokes, A.J., Kurosaki, T.,  
469 Kinet, J.P., et al. 2001. LTRPC7 is a Mg.ATP-regulated divalent cation channel  
470 required for cell viability. *Nature*. **411**(6837): 590-595. doi:10.1038/35079092.  
471 PMID:11385574.
- 472 Piper, H.M. 2000. The calcium paradox revisited: an artefact of great heuristic value.  
473 *Cardiovasc Res*. **45**(1): 123-127. doi:10.1016/s0008-6363(99)00304-1.  
474 PMID:10728324.
- 475 Qin, X., Yue, Z., Sun, B., Yang, W., Xie, J., Ni, E., Feng, Y., Mahmood, R., et al. 2013.  
476 Sphingosine and FTY720 are potent inhibitors of the transient receptor potential  
477 melastatin 7 (TRPM7) channels. *Br J Pharmacol*. **168**(6): 1294-1312.  
478 doi:10.1111/bph.12012. PMID:23145923.
- 479 Sameshima, H., Ota, A. & Ikenoue, T. 1999. Pretreatment with magnesium sulfate protects  
480 against hypoxic-ischemic brain injury but postasphyxial treatment worsens brain  
481 damage in seven-day-old rats. *Am. J. Obstet. Gynecol*. **180**(3 Pt 1): 725-730.  
482 doi:10.1016/s0002-9378(99)70279-6. PMID:10076154.
- 483 Santos-Gallego, C.G., Vahl, T.P., Goliasch, G., Picatoste, B., Arias, T., Ishikawa, K., Njerve,  
484 I.U., Sanz, J., et al. 2016. Sphingosine-1-Phosphate Receptor Agonist Fingolimod  
485 Increases Myocardial Salvage and Decreases Adverse Postinfarction Left Ventricular  
486 Remodeling in a Porcine Model of Ischemia/Reperfusion. *Circulation*. **133**(10): 954-  
487 966. doi:10.1161/CIRCULATIONAHA.115.012427. PMID:26826180.
- 488 Schmouder, R., Serra, D., Wang, Y., Kovarik, J.M., Dimarco, J., Hunt, T.L. & Bastien, M.C.  
489 2006. FTY720: placebo-controlled study of the effect on cardiac rate and rhythm in  
490 healthy subjects. *J. Clin. Pharmacol*. **46**(8): 895-904. doi:10.1177/0091270006289853.  
491 PMID:16855074.

- 492 Suleiman, M.S. & Chapman, R.A. 1993. Calcium paradox in newborn and adult guinea-pig  
493 hearts: changes in intracellular taurine and the effects of extracellular magnesium. *Exp.*  
494 *Physiol.* **78**(4): 503-516. doi:10.1113/expphysiol.1993.sp003702. PMID:8398104.
- 495 Van Vuuren, D., Marais, E., Genade, S. & Lochner, A. 2016. The differential effects of  
496 FTY720 on functional recovery and infarct size following myocardial  
497 ischaemia/reperfusion. *Cardiovasc J Afr.* **27**(6): 375-386. doi:10.5830/CVJA-2016-039.  
498 PMID:27966000.
- 499 Vessey, D.A., Li, L., Imhof, I., Honbo, N. & Karliner, J.S. 2013. FTY720 postconditions  
500 isolated perfused heart by a mechanism independent of sphingosine kinase 2 and  
501 different from S1P or ischemic postconditioning. *Med Sci Monit Basic Res.* **19**: 126-  
502 132. doi:10.12659/MSMBR.883877. PMID:23567658.
- 503 Wagner, S., Maier, L.S. & Bers, D.M. 2015. Role of sodium and calcium dysregulation in  
504 tachyarrhythmias in sudden cardiac death. *Circ Res.* **116**(12): 1956-1970.  
505 doi:10.1161/CIRCRESAHA.116.304678. PMID:26044250.
- 506 Zimmerman, A.N. 2000. The calcium paradox. *Cardiovasc Res.* **45**(1): 119-121.  
507 doi:10.1016/s0008-6363(99)00323-5. PMID:10728322.

## 508    **Legends to figures**

509    **Fig. 1.** Heart perfusion set up and experimental groups. Schematic diagram of the perfusion  
510    apparatus and drug administration set up (A). Experimental groups as determined by the  
511    cardiac perfusion protocols (B). Each drug, nordihydroguaiaretic acid (NDGA), FTY720 or  
512    vehicle (DMSO) was administered at steady-state, after a period of stabilization.

513    Abbreviation: CP,  $\text{Ca}^{2+}$  paradox.

514

515    **Fig. 2.** Effects of NDGA and FTY720 on  $\text{Ca}^{2+}$  paradox-induced infarcts. Representative  
516    images of 2,3,5-triphenyltetrazolium chloride (TTC) stained mid-ventricular slices of hearts  
517    subjected to various drug treatment- and perfusion protocols (A). Viable myocardium appears  
518    darker (TTC-positive) compared to the myocardium with irreversible infarcts that appears  
519    pale (TTC-negative). Infarct size, expressed as % of total the ventricular area (B). Values are  
520    presented as mean  $\pm$  SEM;  $n = 6$  rats per group;  $***P < 0.001$  vs. control;  $**P = 0.003$  vs.  
521    control;  $##P = 0.001$  vs. CP. Abbreviations: FTY, FTY720; CP,  $\text{Ca}^{2+}$  paradox.

522

523    **Fig. 3.** Effects of NDGA and FTY720 on  $\text{Ca}^{2+}$  paradox-induced hemodynamic changes.  
524    Screenshot images of typical left ventricular (LV) pressure recordings in control- and  $\text{Ca}^{2+}$   
525    paradox hearts (A). Summary data of LV end-diastolic pressure (LVEDP), LV developed  
526    pressure (LVDP), and coronary flow rate (B-D). The parameters were measured at the  
527    beginning (baseline) and at the end of the perfusion protocols from different hearts [ $\circ$ ,  
528    control;  $\bullet$ ,  $\text{Ca}^{2+}$  paradox (CP);  $\square$ , nordihydroguaiaretic acid (NDGA);  $\blacksquare$ , NDGA + CP;  $\Delta$ ,  
529    FTY720 (FTY);  $\blacktriangle$ , FTY720 + CP]. Values are presented as mean  $\pm$  SEM;  $n = 6$  rats per  
530    group;  $***P < 0.001$  for CP vs. control;  $**P = 0.008$  for FTY720 + CP vs. control or  
531     $P = 0.006$  for NDGA + CP vs. control;  $\#P = 0.039$  for FTY720 + CP vs. CP or  $P = 0.020$  for

532 NDGA + CP vs. CP; § $P = 0.029$  for FTY720 + CP vs. CP; n.s., not statistically significant  
533 ( $P = 0.40$ ).

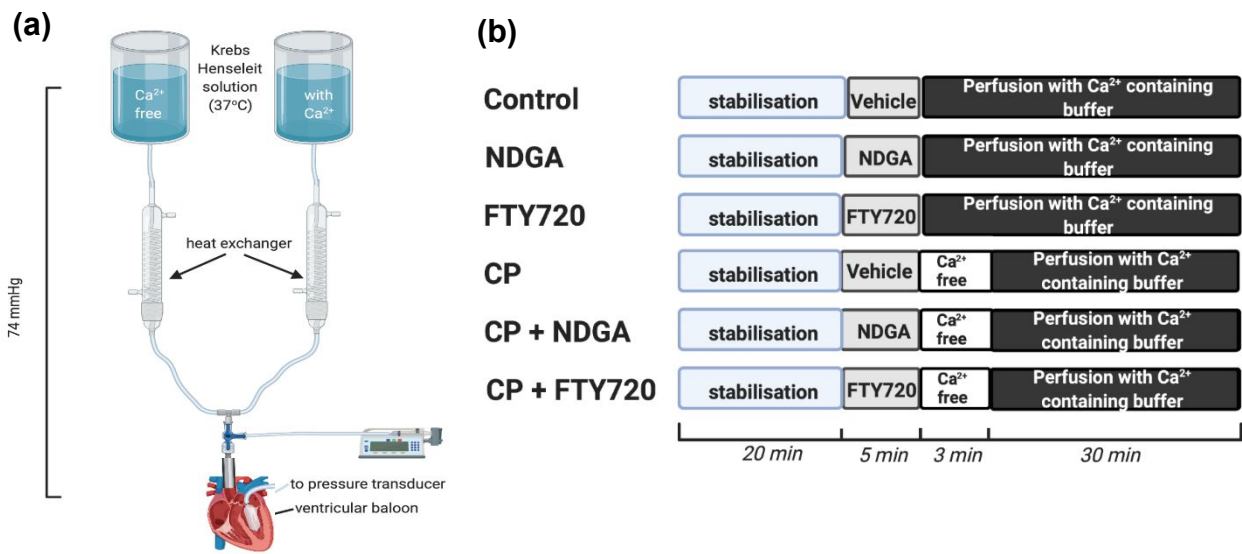
534

535 **Fig. 4.** Effect of  $Mg^{2+}$  pre-treatment on  $Ca^{2+}$  paradox. Experimental groups as determined by  
536 the type of pre-treatment and cardiac perfusion protocols (A). Abbreviations: Mg,  $Mg^{2+}$ ; i.p.,  
537 intraperitoneal; CP,  $Ca^{2+}$  paradox. Representative images of TTC-stained mid-ventricular  
538 slices of hearts from different experimental protocols (B). Infarct size, expressed as % of the  
539 ventricular area (C). Left ventricular (LV) hemodynamic parameters [LV end-diastolic  
540 pressure (LVEDP) and LV developed pressure (LVDP)] measured at baseline and at the end  
541 of the perfusion protocol in the various groups of hearts [ $\circ$ , control;  $\square$ ,  $Mg^{2+}$ ;  $\bullet$ , CP;  $\blacksquare$ ,  $Mg^{2+}$   
542 + CP] (D-E). Values are presented as mean  $\pm$  SEM;  $n \geq 6$  rats per group; \*\*\* $P < 0.001$  for  
543 Mg + CP or CP vs. control; \*\* $P = 0.001$  for Mg + CP vs. control.

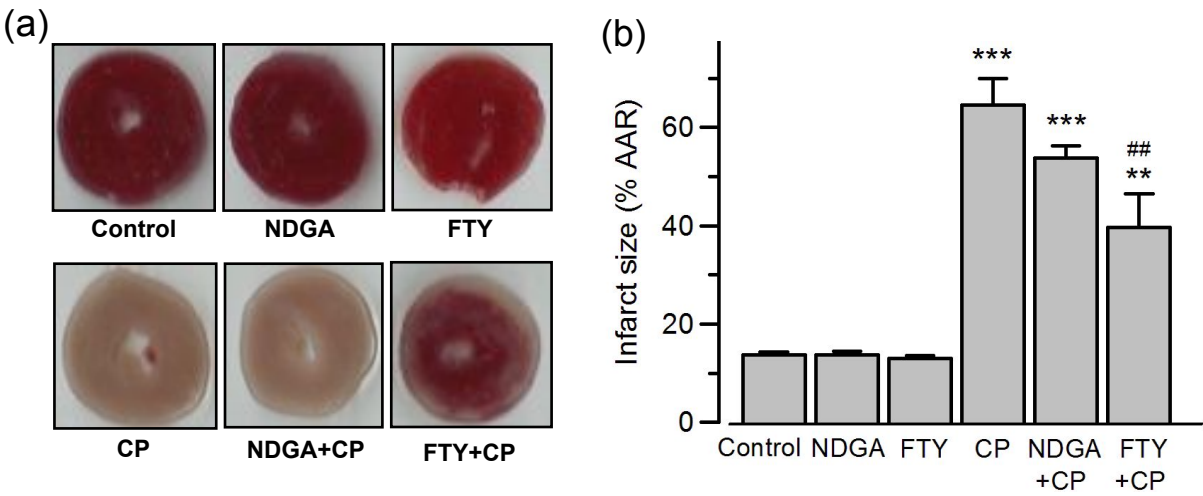
544

545 **Fig. 5.** TRPM7 protein expression in ventricular tissue. Representative Western blot film  
546 images of TRPM7 and  $\beta$ -actin in left ventricular tissue of control (untreated) rats and  $Mg^{2+}$ -  
547 pre-treated rats (A). Summary data of TRPM7 protein expression, relative to that of  $\beta$ -actin  
548 (B). Values are presented as mean  $\pm$  SEM;  $n = 6$  rats per group; n.s., not statistically  
549 significant ( $P = 0.43$ ). Abbreviation: TRPM7, transient receptor potential melastatin 7.

FIGURE 1.



**FIGURE 2.**



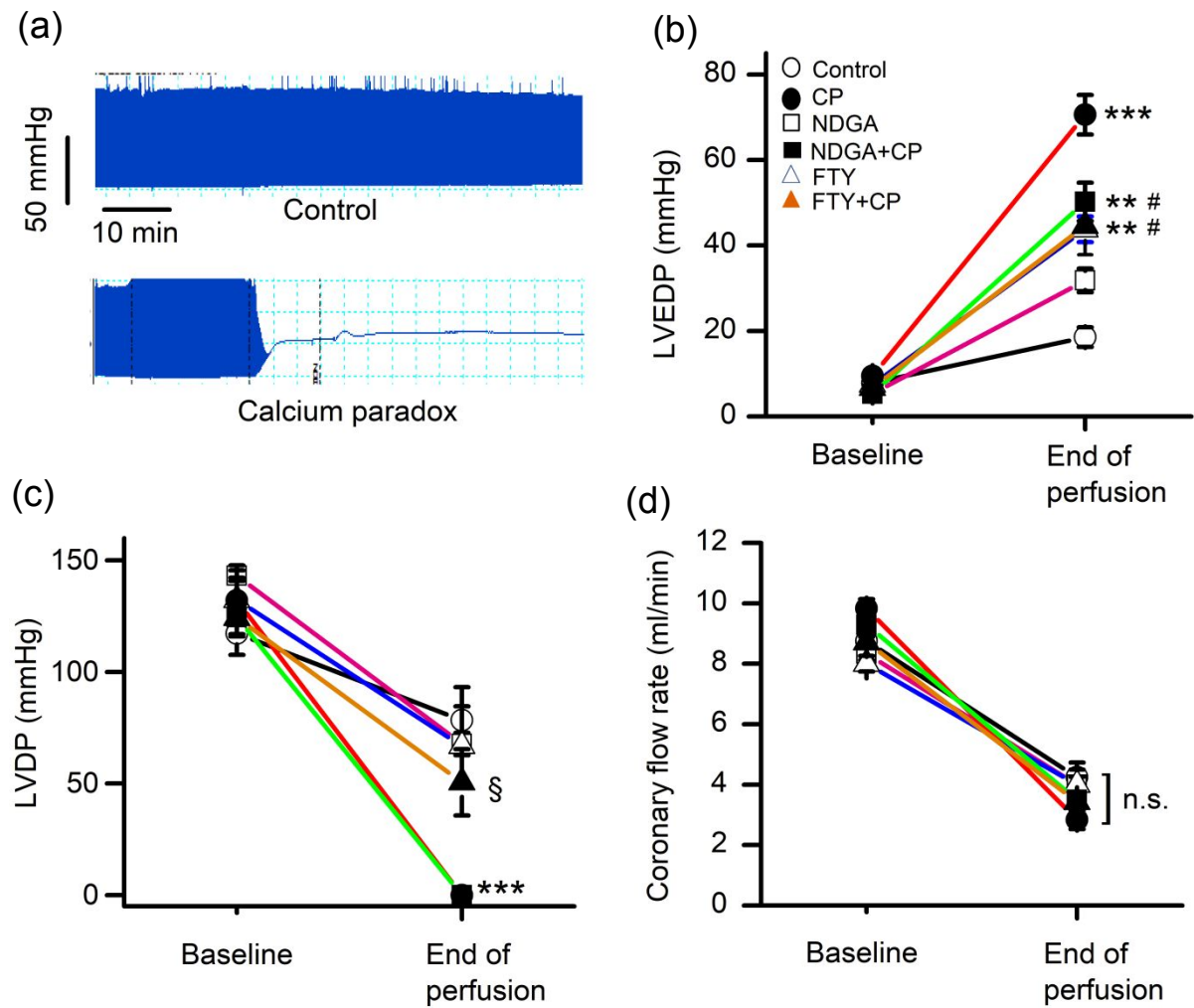
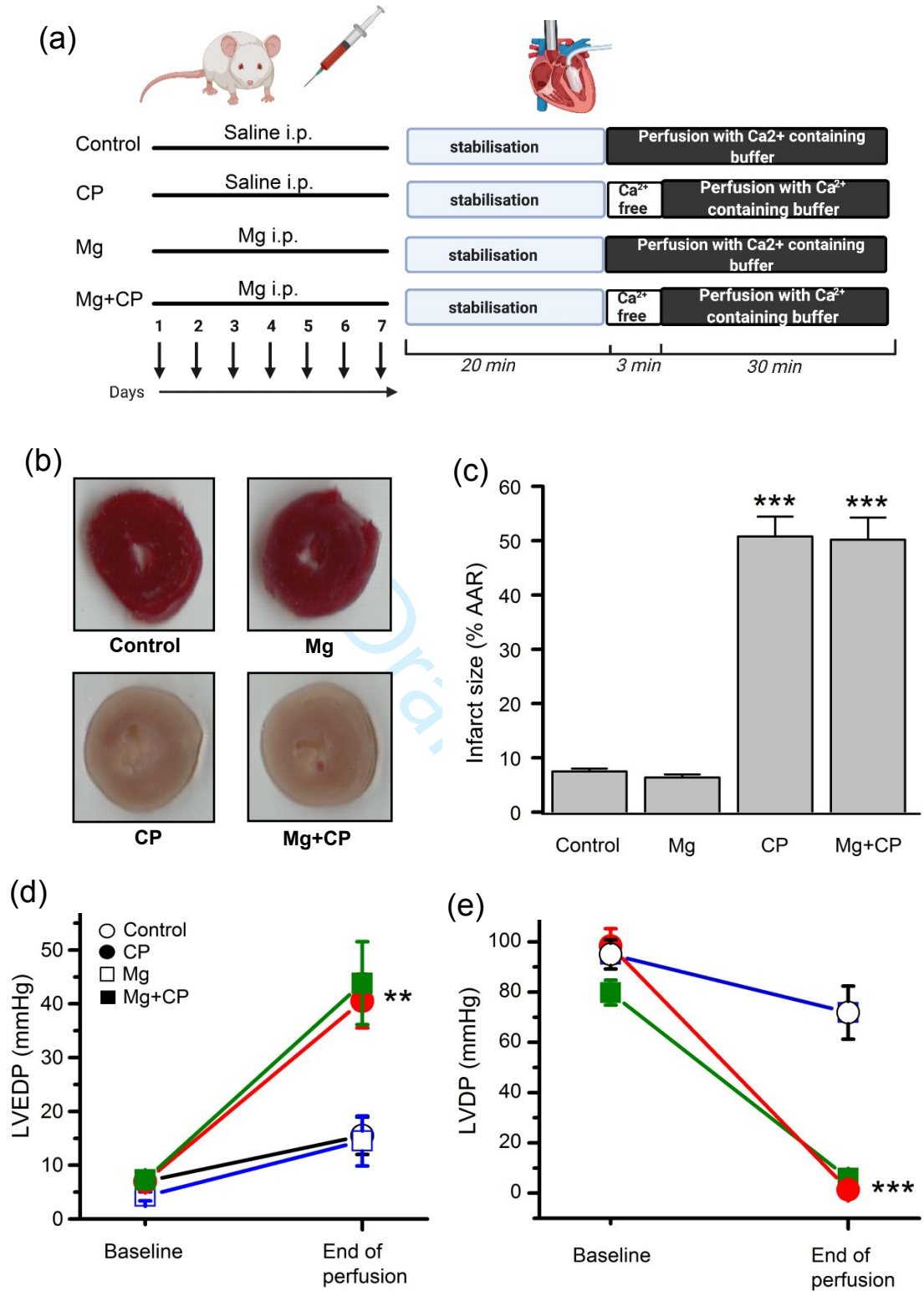
**FIGURE 3.**



FIGURE 4.



**FIGURE. 5**